Archives of Hydro-Engineering and Environmental Mechanics
Vol. 52 (2005), No. 1, pp. 21–37

Simulations of Behaviour of Granular Bodies using a Lattice-Gas Automaton

Jan Kozicki, Jacek Tejchman

Gdańsk University of Technology, Faculty for Civil and Environmental Engineering,
ul. Narutowicza 11/12, 80-952 Gdańsk, Poland, e-mails: janek_k@atelier.pl, tejchmk@pg.gda.pl

(Received November 15, 2004; revised January 17, 2005)

Abstract

A lattice-gas automaton of hydrodynamics was used to calculate the kinematics of non-cohesive granular materials during 3 different complex two-dimensional problems: granular pile, granular flow in a vertical channel and granular flow in a parallel/converging silo. In the model, collisions and dissipation of particles were taken into account. The simulation results were qualitatively compared with experimental results.

Key words: collisions, dissipation, granular flow, gravity, lattice-gas automaton

1. Introduction

The behaviour of granular bodies is highly complex due to their discrete and heterogeneous structure, strong anisotropy, non-linearity and occurrence of strain localisation in the form of shear zones. Different continuum and discrete models are used to describe their behaviour. In continuum mechanics, elasto-plastic (Lade 1977, Vermeer 1982, Pestana and Whittle 1999) and hypoplastic (Darve et al. 1995, Gudehus 1996, Bauer 1996, von Wolffersdorf 1996, Lanier et al. 2004) models are applied. To describe shear localization, continuum models can be extended by micro-polar (Mühlhaus 1990, Tejchman and Wu 1993, Tejchman and Gudehus 2001), non-local (Brinkgreve 1994, Maier 2003, Tejchman 2004), second gradient (Sluys 1992, Pamin 1994, Maier 2003, Tejchman 2004) and viscous terms (Loret and Prevost 1990, Sluys 1992).

In the case of discrete methods, granular dynamics algorithms (Gutfraind and Pouliquen 1996, Luding et al. 1996, Kafui and Thornton1997, Rojek 2003), kinetic theories (Haff 1983, Lun and Savage 1987, Fütterer 1991) and cellular automata (Ulm 1952, Litwiniszyn 1956, Chopard and Droz 1998, Zhou 2004) are applied to capture the salient properties of granulates.

In this paper, a lattice-gas automaton formulated by Frisch et al. (1986) which belongs to the group of cellular automata frequently used in physics, chemistry and biology to describe flow of fluid and gas was used. It has also been used successfully to model the behaviour of granular media (Peng and Herrmann 1994, Alonso and Herrmann 1996, Katsura et al. 2001, Kozicki and Tejchman 2005a), having both advantages and disadvantages relative to other modelling techniques such as FEM or DEM. The advantages include: a large number of particles, lack of restrictions for deformations, implementation simplicity, small amount of computer time needed to describe flow (the behaviour is described not by the terms of differential equations) and consideration of particle collisions and energy dissipation. The disadvantage is that it is a purely kinematic approach (no flow dynamics is involved).

The intention of simulations presented in this paper was to show the capability of a lattice-gas automaton to describe the behaviour of granular materials in 3 different two-dimensional boundary value problems: sandpile, flow in a vertical channel and flow in a silo consisting of parallel and convergent walls. The simulation results were qualitatively compared with corresponding laboratory tests.

2. Characteristics of the Model

In a lattice-gas automaton used in the paper, each site of a hexagonal lattice can be occupied by one or more particles, boundary wall or empty. The particles move on the nearest-neighbour bonds (with unit velocity) and second-nearest neighbours of the lattice (with unit velocity multiplied by the factor $\sqrt{3}$). Each particle at each site has 13 Boolean states which are related to the velocity vectors v_i ($i = 0, 1, 2, ..., 12$), Fig. 1. The direction of motion of a particle v can be towards any of its 12 nearest neighbours ($i = 1, 2, ..., 12$) or be at rest ($v_o = 0$). Thus, at the beginning of calculations, the number of particles per site has a maximum value of 13 and a minimal value of 0. The time evolution consists of one collision step and two propagation steps. In the collision step, the particles both change their velocities due to collisions or remain at rest in the site by losing the total kinetic energy due to dissipation. In the first propagation step, particles without a velocity (more particles than one) are scattered randomly to the nearest empty sites including a low quantity of particles. In the second propagation step, colliding particles (after changing their velocities) are transferred in the direction of their velocities to the nearest sites where they collide again (Fig. 2). In general, collisions conserve mass and momentum. The system is updated in parallel. The following six material parameters were assumed in the model: two collision parameters (p, q), two gravity parameters (g, h) and two friction parameters (b, k). All probabilistic parameters were chosen in the range of from 0 to 1.

The collision parameter p determines the number of particles n, which were at rest after the collision (due to energy dissipation). The parameter n is calculated

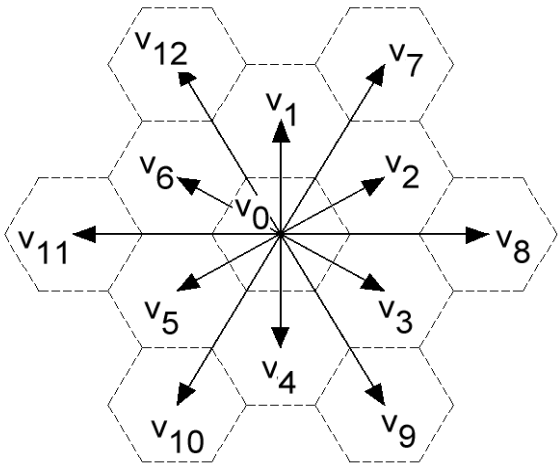

Fig. 1. Vectors of particle velocities at each site (lattice-gas automaton)

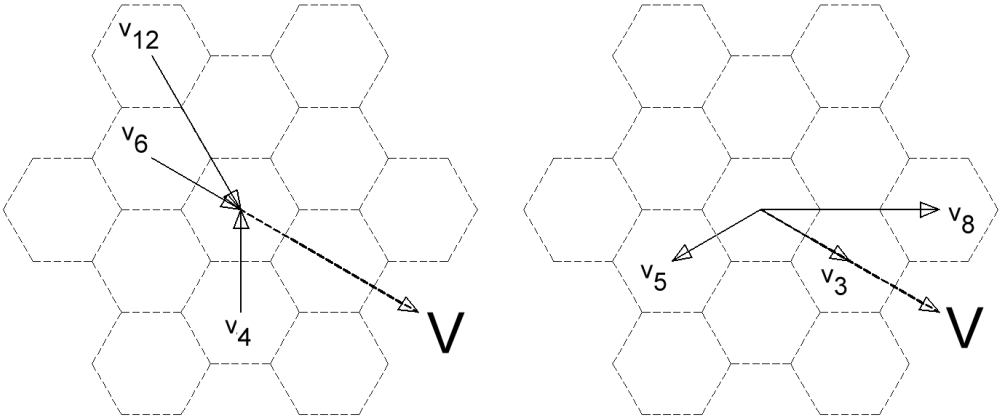

Fig. 2. Examples of calculated velocity vectors for particles after collisions using a lattice-gas automaton (V – resultant velocity)

from the formula $p^{(n+1)} < r_1 < p^n$ (r_1 is a random number). Due to the fact that some particles are stopped after collisions, other particles can leave the sites at a higher velocity due to the conservation of momentum. When more than one particle is stopped and the conservation of momentum can not be fulfilled, the particles move in random directions. In turn, the parameter q describes the loss of energy during each collision. The number of random particles l (which are not considered when calculating the resultant velocity) is obtained from the formula $q^{(l+1)} < r_2 < q^l$ (r_2 is a random number). Due to the loss of energy, the particles leave the sites at a lower velocity. The total number of possible combinations for collisions is equal to $2^{12} = 4096$ and the number of possible velocity directions is 108. To speed up the calculation process, the appropriate table of collisions has been generated (Fig. 3). If parameters p and q are equal to zero, the sum of outgoing velocity vectors from each site is equal to the sum of incoming velocity vectors (elastic collisions take place).

The gravity parameter g is taken into account during each collision in such a way that the vertical velocity v_4 (Fig. 1) is added to the resulting velocity vector of outgoing particles with a probability of g. Thus, the particles are accelerated downwards after each collision. In turn, the gravity parameter h is introduced to improve the direction of the resultant velocity vector so that the direction would become parabolic for single particles (Fig. 4). The particle at rest at the given site (v_0) can move downwards to the state v_0 in the neighboring empty site without any velocity in only one of the chosen directions v_3, v_4, v_5, v_9 and v_{10} (Fig. 1). If $h = 1$, particles without velocities move downwards (density becomes more uniform). In turn, if $h = 0$, particles without velocities do not move.

The friction parameter k describes the internal interaction between particles. If the parameter k is different from zero, certain migration directions become dominant (to induce movement in one specific direction). In our simulations, the horizontal direction is assumed to be dominant. Thus, the resulting velocity vector of outgoing particles is replaced by the sum of random velocity vectors in directions v_2, v_3, v_5, $v_{6,}$, v_8 and v_{11} with a probability of k (Fig. 1). The friction parameter b describes the wall roughness. If particles hit the wall, they are stopped with a probability of b (the increase of wall roughness corresponds to the increase of parameter b). Afterwards, they are scattered randomly to the nearest empty sites with low contents of particles.

The initial density of the granulate is generated at the onset of flow depending upon parameters p, q, g and k. The density increases with increasing p and g and decreasing q and k.

The model used is based on the lattice-gas automaton proposed for granular materials by Peng and Herrmann (1994) and Alonso and Herrmann (1996). However, it includes some improvements. The innovations are the following: the model is also applied to silo flow, the number of possible vector directions is enhanced (13 instead of 7), material density is not used as an additional parameter,

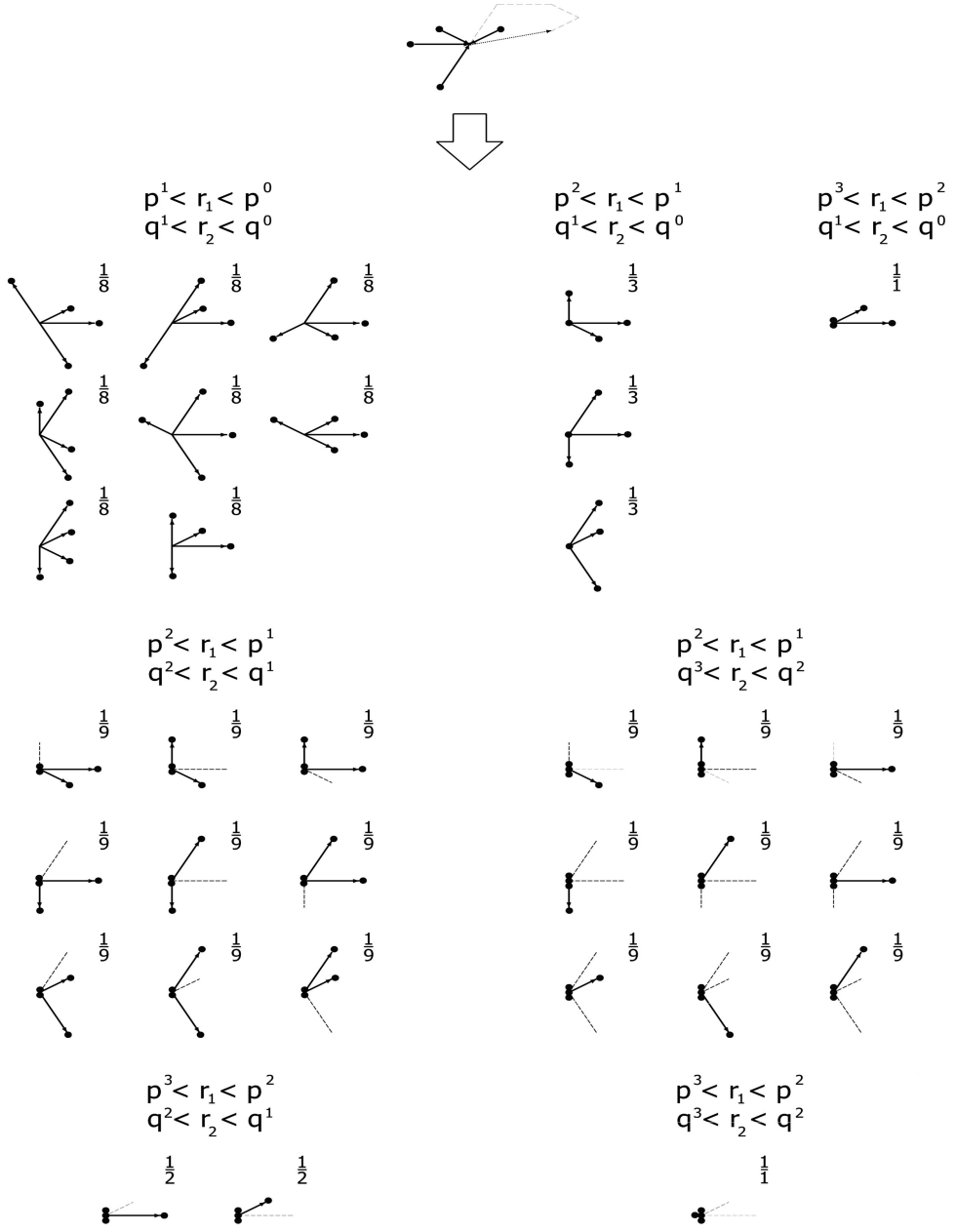

Fig. 3. Examples of collision rules for 4 particles flowing to one random site (arrows represent the directions of moving particles and full dots stand for particles)

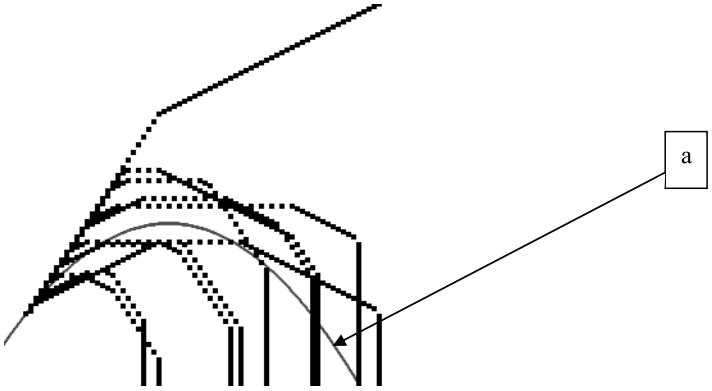

Fig. 4. Examples of calculated traces of single particles in the gravity field thrown from the same point in the direction of v_7 of Fig. 1 (line *a* denotes a parabolic trajectory)

gravitation is depicted with two parameters (instead of one), rough walls are able to stop flowing particles, the method describing collisions enables any number of particles to stop, and the new parameter is introduced to describe the internal interaction between particles.

During simulations, the following values of the material parameters were assumed: $p = 0.2$, $q = 0.2$, $b = 0.05$, $k = 0.05$, $g = 0.2$ and $h = 0.05$.

3. Results

3.1. Granular Pile

The 2D-results of simulations of a granular pile including 15000 cells (particles) are demonstrated in Fig. 5. During the simulation, the particles were slowly added at a fixed rate from the top of the system to the bottom. Gravity moved these particles down until they collided with a rigid wall at the bottom, then forming a heap.

The profile of the heap created is similar to a cone with a well defined angle of repose equal to 30° (determined by the geometry of the underlying lattice). As compared with a perfect cone, it shows, however, small kinks along the surface and a slightly curved tail (with a slope inclination of less than 30°) which is in accordance with the experimental results by Alonso and Herrmann (1996).

3.2. Granular Flow in a Vertical Channel

The time evolution of the density in a vertical channel during 2D-simulations with 35000 cells is demonstrated in Fig. 6. Periodic boundary conditions were used in

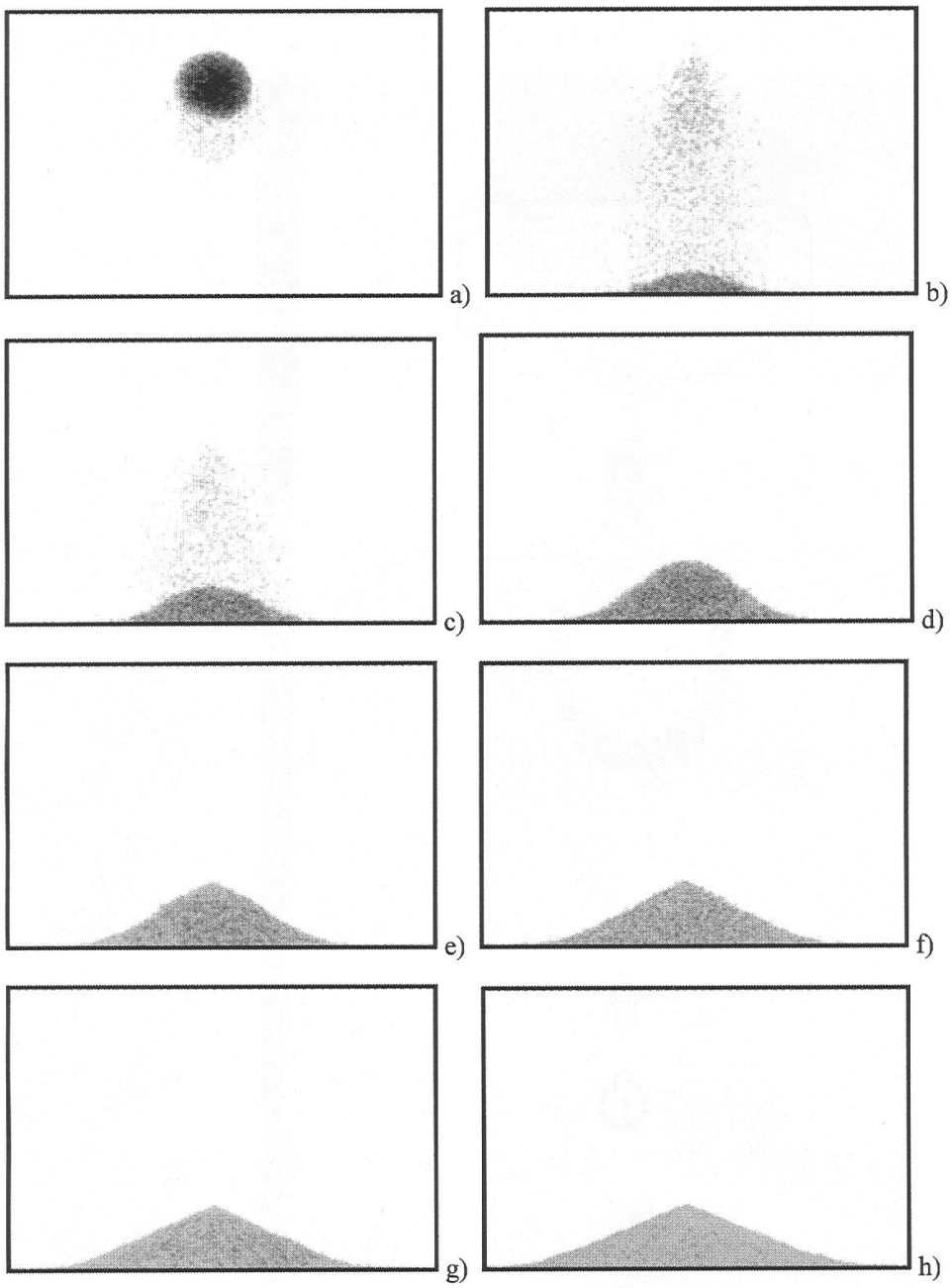

Fig. 5. Formation of a granular pile in the iteration: a) 60, b) 180, c) 300, d) 420, e) 720, f) 1020, g) 1320 and h) 1800

the vertical direction. In this way, the channel was continuously filled. The darker regions are associated with higher densities, and the lighter regions are associated with lower densities of the silo fill.

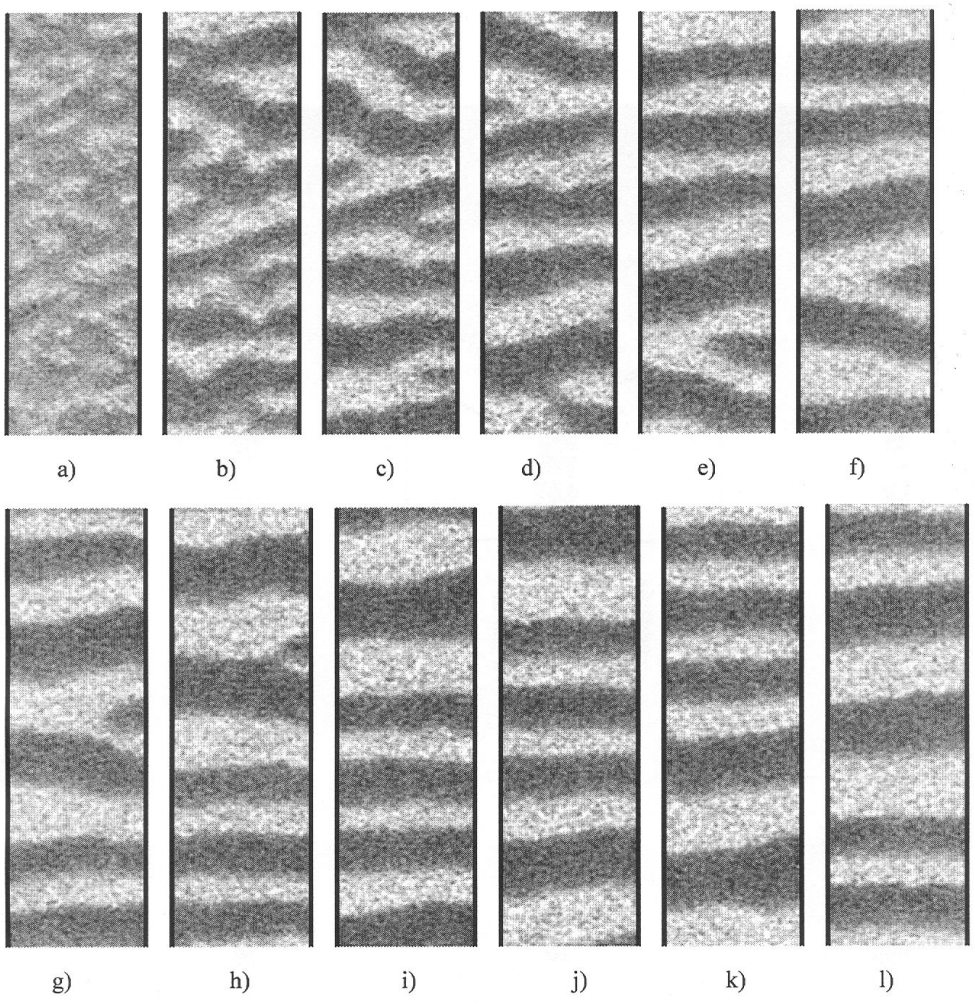

Fig. 6. Evolution of density waves during granular flow in a vertical channel in the iteration: a) 60, b) 180, c) 300, d) 420, e) 540, f) 660, g) 900, h) 1140, i) 1380, j) 1620, k) 1860 and l) 2160

Initially, the density was overall non-homogeneous. During continuous flow, layers of high and low density were gradually formed out of the system. These layers created permanent density waves. The shape of density waves is in accordance with experiments by Cowin and Comfort (1982) carried out in a rectangular rough-walled cylinder with sand, wherein x-rays were used to detect zones of increased porosity.

The density waves were not numerically obtained during granular flow, if the collisions parameters and the wall roughness parameter were equal to zero.

3.3. Granular Flow in a Silo

The 2D-simulations with a lattice-gas automaton including 35000 cells are demonstrated in Fig. 7 with a mass flow silo and a funnel flow silo. The effect of the parameters *g, h, k, b, p* and *q* is shown only for a mass flow silo (Figs. 8–13); their effect in a funnel flow silo was similar (Kozicki and Tejchman 2005b). For a better comparison, one chose small and large values of these parameters. The following number of iterations was needed to describe the entire process of silo emptying: 5340 (Fig. 7a), 3480 (Fig. 7b), 5520 (Fig. 8a), 8860 (Fig. 8b), 13500 (Fig. 9a), 5160 (Fig. 9b), 7200 (Fig. 10a), 5340 (Fig. 10b), 5340 (Fig. 11a), 8860 (Fig. 11b), 13320 (Fig. 12a), 5460 (Fig. 12b), 6780 (Fig. 13a) and 5400 (Fig. 13b).

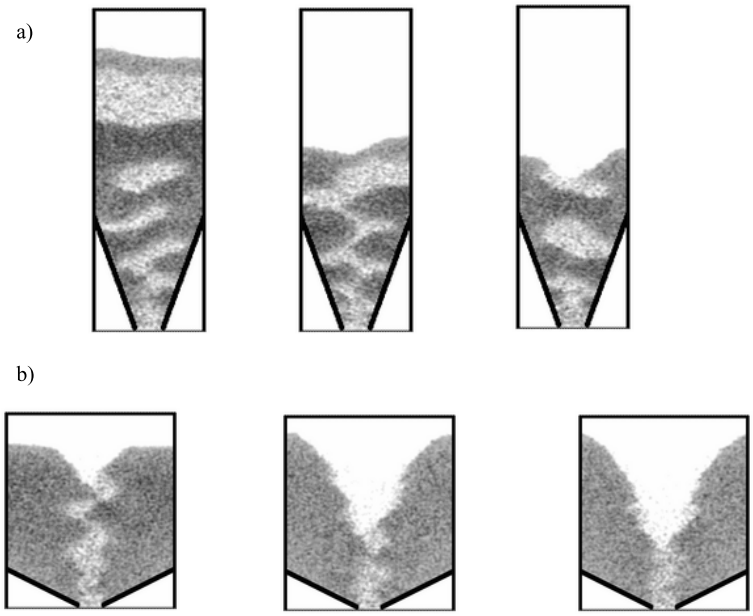

Fig. 7. Evolution of density waves during granular flow in a mass (a) and funnel (b) flow model silo

In all cases, regions with a different density occur during granular flow. The flow is non-symmetric. The shape of dilatant zones is strongly influenced by the collision parameter p and gravity parameter h. In a mass flow silo, it is also dependent upon the wall roughness parameter b (more particles were stopped at the wall). With decreasing collision parameter p, the height of dilatant zones significantly increases (material behaves more as gas). If the gravity parameter h is large, the dilatant zones become narrower and are more concentrated in the

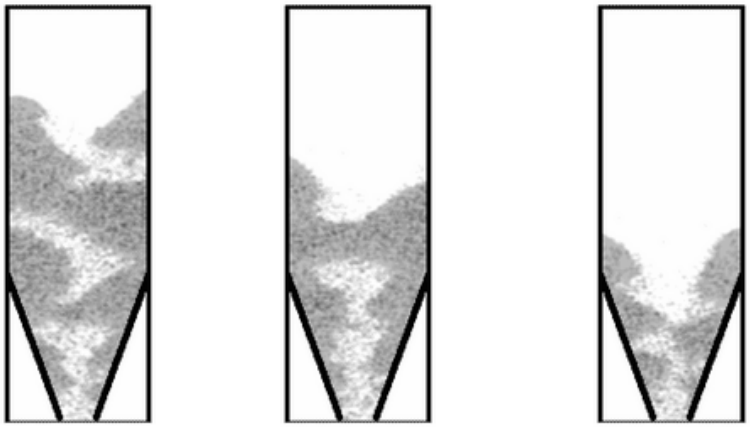

Fig. 8. Flow pattern in a mass flow silo (effect of the gravity parameter g):
a) $p = 0.2$, $q = 0.2$, $b = 0.05$, $k = 0.05$, $g = 0.95$, $h = 0.05$,
b) $p = 0.2$, $q = 0.2$, $b = 0.05$, $k = 0.05$, $g = 0.05$, $h = 0.05$

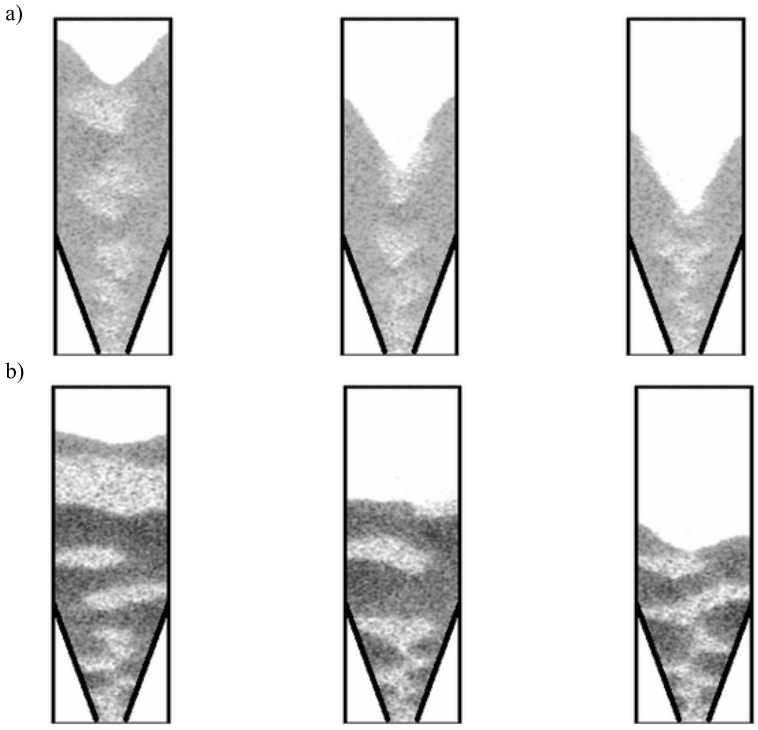

Fig. 9. Flow pattern in a mass flow silo (effect of the gravity parameter h):
a) $p = 0.2$, $q = 0.2$, $b = 0.05$, $k = 0.05$, $g = 0.2$, $h = 0.8$,
b) $p = 0.2$, $q = 0.2$, $b = 0.05$, $k = 0.05$, $g = 0.2$, $h = 0.0$

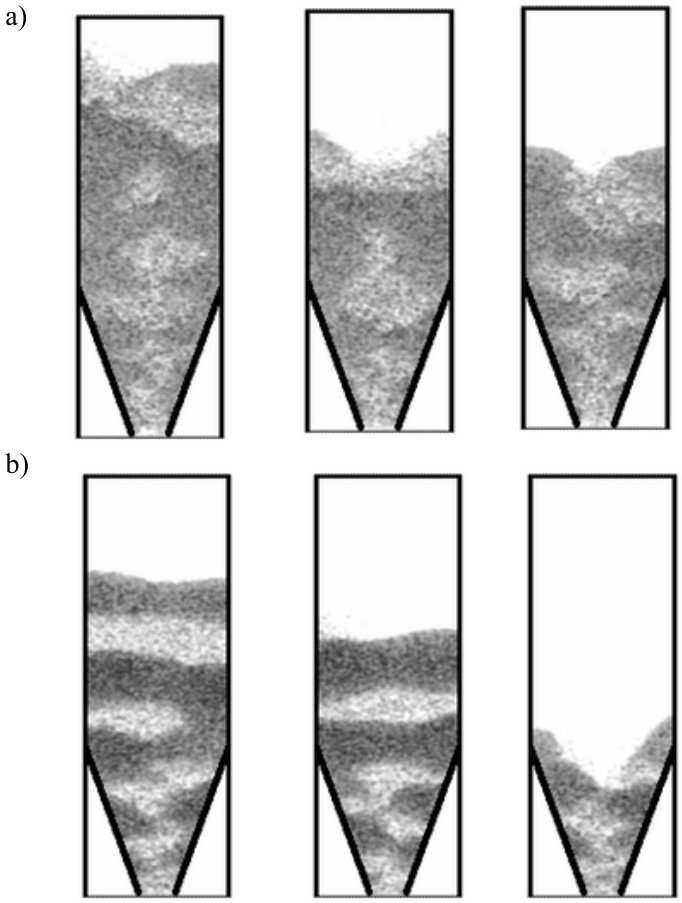

Fig. 10. Flow pattern in a mass flow silo (effect of the friction parameter k):
a) $p = 0.2$, $q = 0.2$, $b = 0.05$, $k = 0.8$, $g = 0.2$, $h = 0.05$,
b) $p = 0.2$, $q = 0.2$, $b = 0.05$, $k = 0.0$, $g = 0.2$, $h = 0.05$

mid-region of the silo due to the fact that there are more empty sites in the middle of the silo than close to the walls.

For a smaller wall roughness parameter b, the dilatant zones are more horizontal since the flow disturbance close to walls is smaller. The outflow rate increases obviously with increasing gravity parameter g. With an increase of the gravity parameter g, the effect of other factors also becomes insignificant. The inclination of the upper free surface of the material decreases with decreasing parameters p, q and h (material behaves more as gas). The non-uniformity of the material density increases with increasing parameter g and decreasing parameters h, k, p and q.

The calculated flow patterns in both silos are in satisfactory agreement with the experimental ones (Kozicki and Tejchman 2001). The shape of the propagating

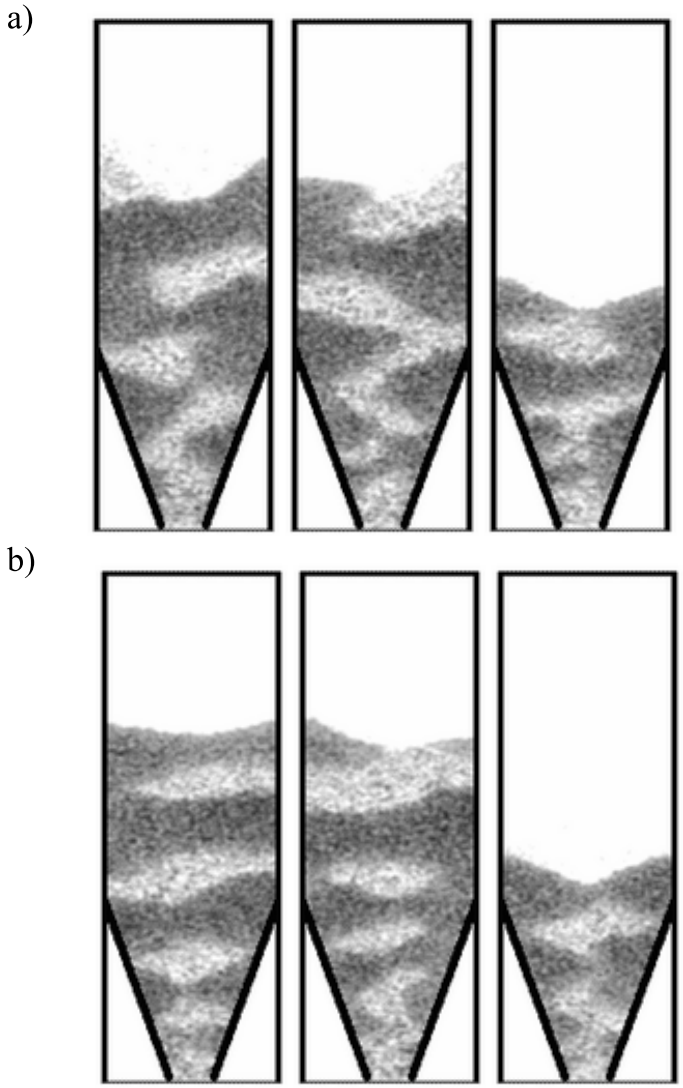

Fig. 11. Flow pattern in a mass flow silo (effect of the wall roughness parameter b):
a) $p = 0.2$, $q = 0.2$, $b = 0.8$, $k = 0.05$, $g = 0.2$, $h = 0.05$,
b) $p = 0.2$, $q = 0.2$, $b = 0.0$, $k = 0.05$, $g = 0.2$, $h = 0.05$

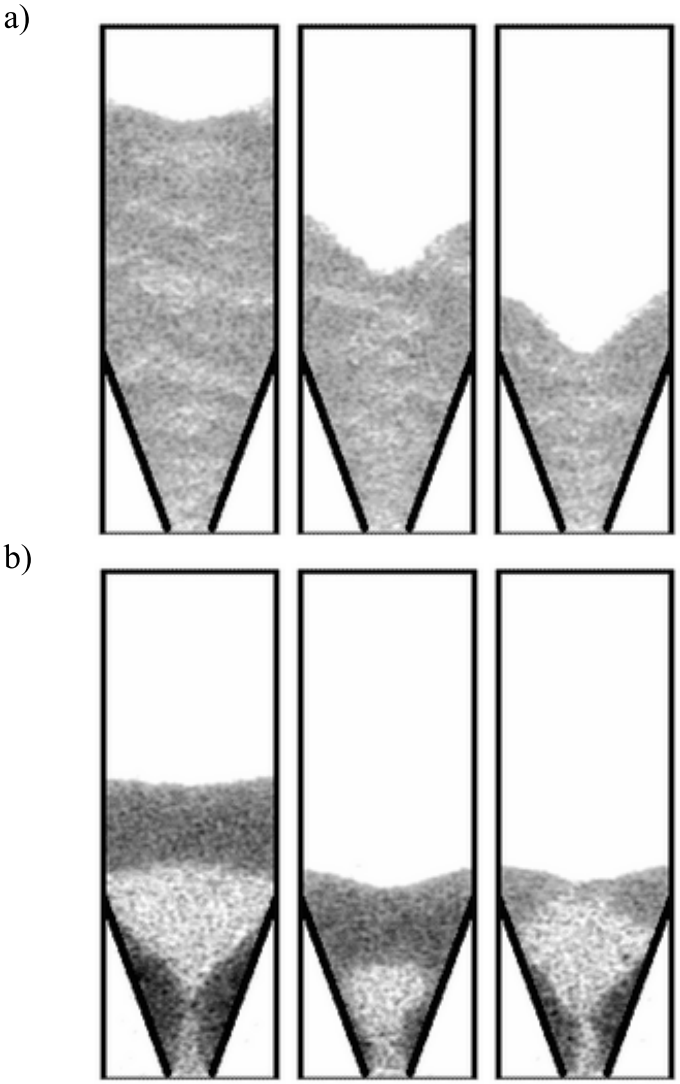

Fig. 12. Flow pattern in a mass flow silo (effect of the collision parameter p):
a) $p = 0.8$, $q = 0.2$, $b = 0.05$, $k = 0.05$, $g = 0.2$, $h = 0.05$,
b) $p = 0.0$, $q = 0.2$, $b = 0.05$, $k = 0.05$, $g = 0.2$, $h = 0.05$

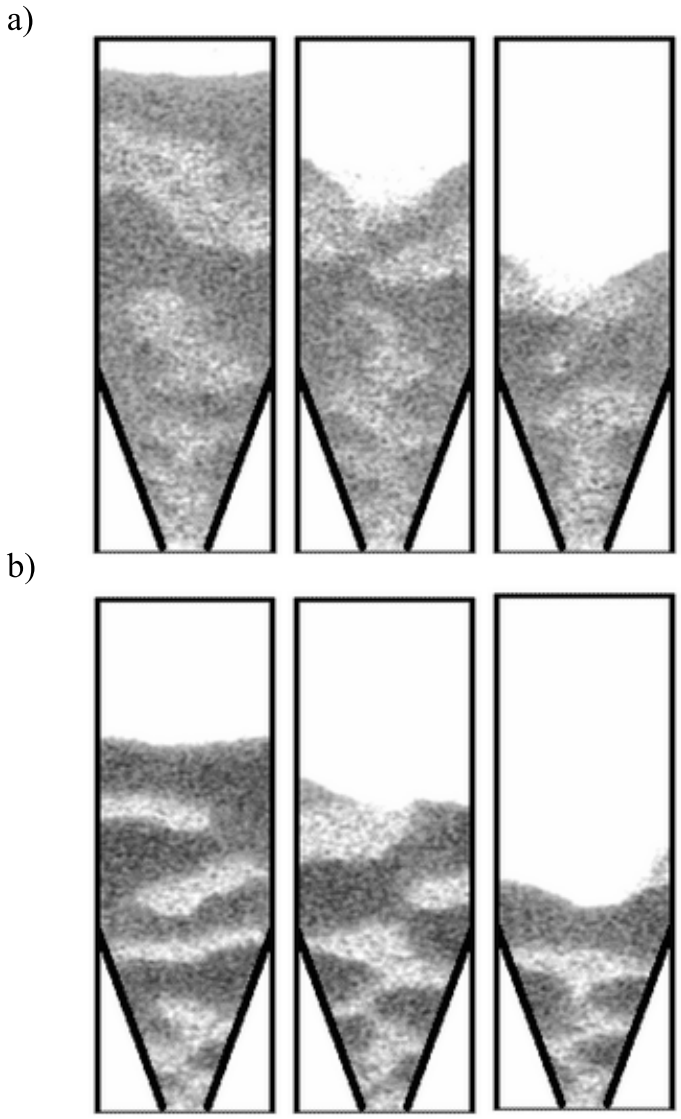

Fig. 13. Flow pattern in a mass flow silo (effect of the collision parameter q):
a) $p = 0.2$, $q = 0.8$, $b = 0.05$, $k = 0.05$, $g = 0.2$, $h = 0.05$,
b) $p = 0.2$, $q = 0.0$, $b = 0.05$, $k = 0.05$, $g = 0.2$, $h = 0.05$

dilatant zones inside the flowing material is similar to the experimental results by Lavrikov and Revuzhenko (1990). However, it differs from the experimental ones by Michalowski (1984, 1990) where a symmetrical pair of curvilinear dilatant rupture zones was created in the neighbourhood of the outlet during mass flow. The zones propagated upward, crossed each other around the symmetry of the silo, reached the walls and were subsequently reflected from them. This process repeated itself until the zones reached the free boundary in the converging hopper or the transition zone in the parallel-converging silo. In the case of a funnel flow silo, the curvilinear dilatant zones in the material core were symmetric about a vertical mid-line. Some of them crossed each other.

4. Conclusions

The lattice-gas automaton is a purely kinematic discrete model wherein flow dynamics is not taken into account. It offers the advantage of the guaranteed numerical stability coupled with the extreme computational simplicity. Despite this simplicity, it is apt to realistically describe the behaviour of granular materials. The calculated shape of granular heaps and density waves in a vertical channel were similar to those in the experiment. The form of the flow pattern in a silo was also realistic. However, the shape of density waves in a silo fill affected by gravity, collision and friction parameters was different from that obtained in some laboratory experiments.

Further numerical studies checked with experiments are necessary to verify the model.

References

Alonso J. J., Herrmann H. J. (1996), Shape of the Tail of a Two-Dimensional Sandpile, *Physical Review Letters*, **76**, 26, 4911–4914.

Bauer E. (1996), Calibration of a Comprehensive Hypoplastic Model for Granular Materials, *Soils and Foundations*, **36,** 1, 13–26.

Brinkgreve R. (1994), Geomaterial Models and Numerical Analysis of Softening, *Dissertation*, Delft University, 1–153.

Chopard B., Droz M. (1998), *Cellular Automata Modelling of Physical Systems*, Cambridge University Press.

Cowin S. C., Comfort W. J. (1982), Gravity-Induced Density Discontinuity Waves in Sand Columns, *J. of Applied Mechanics*, 49, 497–500.

Darve F., Flavigny E., Megachou M. (1995), Yield Surfaces and Principle of Superposition Revisited by Incrementally Non-Linear Constitutive Relations, *Int. J. Plasticity*, **11**, 8, 927–948.

Frisch U., Hasslacher B., Pomeau Y. (1986), Lattice-Gas Automata for the Navier-Stokes Equation, *Physical Review Letters*, 56, 1505–1508.

Fütterer G. (1991), Untersuchungen zum Schnellen Fließen von Trockenen, Kohäsionslosen Schüttgütern in Konvergenten Schächten. *Dissertation,* Karlsruhe University.

Gudehus G. (1996), A Comprehensive Constitutive Equation for Granular Materials, *Soils and Foundations*, **36,** 1, 1–12.

Gutfraind R., Pouliquen O. (1996), Study of the Origin of Shear Zones in Quasi-Static Vertical Chute Flows by using Discrete Particle Simulations, *Mechanics of Materials*, **24**, 273–285.

Haff P. K. (1983), Grain Flow as a Fluid-Mechanical Phenomenon, *J. Fluid Mech*, **134**, 401–430.

Kafui K. D., Thornton C. (1997), Some Observations on Granular Flow in Hoppers and Silos, [in:] *Powders and Grains* (eds.: Behringer and Jenkins), Balkema, Rotterdam, 511–514.

Katsura N., Shimosaka A., Shirakawa Y., Hidaka J. (2001), Simulation for Flow Behaviour of Vibrating Granular Materials Using Cellular Automata, [in:] *Powders and Grains* (ed. Kishino, Swets and Zeitlinger), Lisse, 525–528.

Kozicki J., Tejchman J. (2001), Simulations of Granular Flow in Silos with a Cellular Automata Model, *The International J. of Storing, Handling and Processing Powder*, **13**, 3, 267–275.

Kozicki J., Tejchman J. (2005a), Application of a Cellular Automaton to Simulations of Granular Flow in Silos, *Granular Matter* (under press).

Kozicki J., Tejchman J. (2005b), Simulations of Flow Patterns in Silos with a Cellular Automation – part 2, *Task Quarterly*, **9**, 1, 103–115.

Lade P. V. (1977), Elasto-Plastic Stress-Strain Theory for Cohesionless Soil with Curved Yield Surfaces, *Int. J. Solid Structures*, **13**, 1019–1035.

Lanier J., Caillerie D., Chambon R. (2004), A General Formulation of Hypoplasticity, *Int. J. Numer. Anal. Methods in Geomech.*, **28**, 15, 1461–1478.

Lavrikov S. W., Revuzhenko A. F. (1990), Calculations of Shear Localization in Bulk Solids in Radial Channels, *Fiz.-Tekh. Probl. Razrab. Polezn*, **1**, 3–9 (in Russian).

Litwiniszyn J. (1956), Application of the Equation of Stochastic Processes to Mechanics of Loose Bodies, *Archives of Applied Mechanics*, **8**, 4, 393–411.

Loret B., Prevost J. H. (1990), Dynamic Strain Localisation in Elasto-Visco-Plastic Solids, Part 1, General Formulation and One-Dimensional Examples, *Comp. Appl. Mech. Eng.,* **83**, 247–273.

Luding S., Duran J., Clement E., Rejchenbach J. (1996), Computer Simulations and Experiments of Dry Granular Media: Polydisperse Disks in a Vertical Pipe, *Proc. 5th World Congress of Chemical Engineering*, San Diego, 5, 325–330.

Lun C. K. K., Savage S. B. (1987), A Simple Kinetic Theory for Granular Flow of Rough, in Elastic Spherical Particle, *J. Appl. Mech*, **54,** 47–53.

Maier T. (2003), Non-Local Modelling of Softening in Hypoplasticity, *Comput. Geotech*, **30,** 7, 599–610.

Michalowski R. L. (1984), Flow of Granular Material Through a Plane Hopper, *Powder Technology*, **39,** 29–40.

Michalowski R. L. (1990), Strain Localization and Periodic Fluctuations in Granular Flow Processes from Hoppers, *Geotechnique*, **40**, 3, 389–403.

Mühlhaus H.-B. (1990), Continuum Models for Layered and Blocky Rock, [in:] *Comprehensive Rock Engineering* (eds: J. A. Hudson and Ch. Fairhurst), Pergamon Press, **2**, 209–231.

Pamin J. (1994), Gradient-Dependent Plasticity in Numerical Simulation of Localisation Phenomena, *PhD Thesis*, Delft University, 1–134.

Peng G., Herrmann H.J. (1994), Density Waves of Granular Flow in a Pipe Using Lattice Gas Automata, *Phys. Rev.*, **49**, 3, 1796–1799.

Pestana J. M., Whittle A. J. (1999), Formulation of a Unified Constitutive Model for Clays and Sands, *In. J. Num. Anal. Meth. Geomech.*, **23**, 1215–1243.

Rojek J. (2003), Numerical Modelling and Simulation of the Moulding Process of Sand Forms with a Method of the Lost Model, *Informatyka w Technologii Materiałów*, **3**, 113–125.

Sluys L. Y. (1992), Wave Propagation, Localisation and Dispersion in Softening Solids, *PhD Thesis*, Delft University of Technology.

Tejchman J., Wu W. (1993), Numerical Study on Shear Band Patterning in a Cosserat Continuum, *Acta Mechanica*, **99**, 61–74.

Tejchman J., Gudehus G. (2001), Shearing of a Narrow Granular Strip with Polar Quantities, *J. Num. and Anal. Methods in Geomechanics*, **25**, 1–18.

Tejchman J. (2004), Influence of a Characteristic Length on Shear Zone Thickness in Hypoplasticity with Different Enhancements, *Computers and Geotechnics* (in print).

Ulm S. (1952), Random Processes and Transformations, *Proc. Int. Con. Math.*, **2**, 264–275.

Vermeer P. (1982), A Five-Constant Model Unifying Well-Established Concepts, *Proc. Int. Workshop on Constitutive Relations for Soils* (eds. G. Gudehus, F. Darve and I. Vardoulakis), Balkema, 175–197.

von Wolffersdorff P. A. (1996), A Hypoplastic Relation for Granular Materials with a Predefined Limit State Surface, *Mechanics Cohesive-Frictional Materials*, **1**, 251–271.

Zhou J. G. (2004), *Lattice Boltzman Methods*, Springer Verlag.